IOP Conference Series: Materials Science and Engineering

PAPER • **OPEN ACCESS**

Application of a generalized compressor modeling framework for simulating an oil-injected twin-screw compressor

To cite this article: Nicholas Salts *et al* 2019 *IOP Conf. Ser.: Mater. Sci. Eng.* **604** 012009

View the article online for updates and enhancements.

This content was downloaded from IP address 123.113.27.253 on 15/10/2019 at 20:38

IOP Conf. Series: Materials Science and Engineering **604** (2019) 012009 doi:10.1088/1757-899X/604/1/012009

Application of a generalized compressor modeling framework for simulating an oil-injected twin-screw compressor

Nicholas Salts[1], Davide Ziviani[1], Eckhard A. Groll[1]

[1]Purdue University, School of Mechanical Engineering, Ray W. Herrick Laboratories, West Lafayette, IN, USA

E-mail: nsalts@purdue.edu,dziviani@purdue.edu, groll@purdue.edu

Abstract. Oil-injected twin-screw compressors are widely employed in many commercial and industrial applications because of their high efficiency and reliability. Although extensive literature on modeling techniques applied to twin-screw machines exists, researchers are continuously developing models to capture advanced physical phenomena occurring during the compression process (*e.g.*, mass and heat transfer mechanisms). In order to generalize the concept of mechanistic compressor modeling, a framework for the simulation of positive displacement compressors and expanders (PDSim) has been developed and validated by the authors. The platform has been utilized to model a number of compressor types including scroll, reciprocating, linear, single-screw, rolling-piston, Z, and spool. In this work, the simulation tool has been extended to include twin-screw machines. Beside the detailed geometry model needed to obtain volume curves of the working chambers, sealing lines, and rotor surface areas, three main aspects have been enhanced with respect to the existing literature: (i) a two-fluid (refrigerant and lubricant oil) chamber model with mass and heat transfer interactions; (ii) computation of gas forces, loads on the bearings, and hydrodynamic bearing sub-models; (iii) detailed overall energy balance with a multi-lumped temperature thermal network and a discharge gas pulsations post-processing model. A 4/6 oil-injected twin-screw compressor has been considered to conduct experimental analyses with internal pressure and force sensors, modeling and validation as well as sensitivity analyses.

1. Introduction

The twin-screw compressor is a positive displacement rotary machine with helical-like compression chambers. Over the years, various types of twin-screw compressors have been designed and developed in order to optimize their operation. Research studies focused on both thermodynamic aspects (e.g., 1D/3D models, volume ratio control, oil injection) and manufacturing (*e.g.*, profile generation, optimization of contact lines). The male and female rotors are the main components of a twin-screw compressor and they function as both a compression mechanism and a gear pair. The derivation of the profile generation based on different methods has been widely covered in the literature. For example, Tang [1] provided the detailed mathematical formulation of the two-dimensional and three-dimensional envelope method applied to the SRM-D profile. Stosic et al. [2] reviewed the most popular rotor profiles, including the N-rack profile, and their elementary curves.


Content from this work may be used under the terms of the Creative Commons Attribution 3.0 licence. Any further distribution of this work must maintain attribution to the author(s) and the title of the work, journal citation and DOI.
Published under licence by IOP Publishing Ltd

Nomenclature

h	Specific Enthalpy (kJ/kg)
m	Mass (kg)
N	Rotational Speed (rpm)
$\dot{m}$	Mass Flow Rate (kg/s)
p	Pressure (kPa)
$\dot{Q}$	Heat Rate (kW)
R_{ab}	Thermal Resistance (K/kW)
T	Temperature (K)
u	Specific Internal Energy (kJ/kg)
v	Specific Volume (m^3/kg)
V	Volume (m^3)
$\dot{W}$	Power (W)
z	Number of Lobes (-)
$\eta_{is,oa}$	Overall Isentropic Efficiency (-)
η_v	Volumetric Efficiency (-)
ρ	Density (kg/m^3)
θ	Rotation Angle (rad)
ω	Angular Speed (rad/s)
τ	Torque (Nm)

Subscript

1	male
2	female
amb	ambient
CV	Control Volume
comp	compressor
dis	discharge
fr	friction
loss	losses
ref	refrigerant
suc	suction
sh	shaft
th	theoretical

A detailed example of Normal-Rack (N-Rack) profile generation has been published by Wu and Fong [3, 4] including the explicit equations for the 9 curves that formed the rack. A method for the generation of the profile of twin-screw compressor rotor from a meshing line has also been proposed and analytically derived by Zaytsev and Ferreira [5].

The kinematics model of the meshing profiles is the first step to compute the cavity volumes of the working chambers that are necessary to develop detailed mechanistic models of twin-screw machines [1, 6]. In particular, a number of comprehensive models are reported in the literature with different levels of complexity. The thermodynamic aspects need to be linked with the estimation of the forces and moments acting on the rotors as well as on the bearings. For instance, Adams [7] developed a computer model to study the interactions between the rotors and compute the backlash type rotor vibrations (chatter) as well as bearing forces. The forces and moments due to gas compression were computed using vector calculus principles to integrate the chamber pressure over the rotor surfaces. The 3-dimensional surface of each rotor was mapped to a 2-dimensional region. Koai [6] also included the effect of a slide-valve capacity control mechanism. Additional studies that covered the analyses of forces and moments in twin-screw compressors were conducted by You [8] and Tran et al. [9]. The detailed quantification of hydraulic and mechanical losses in an oil-flooded twin-screw expander was performed by Nikolov et al. [10].

In some of these studies, the models were validated by employing internal pressure sensors to reconstruct the indicated diagram of the compression process as well internal temperature measurements. With respect to bearing loads, Hou et al. [11] conducted an experimental study on the axial force on the rotors of a twin-screw compressor operating at high pressures such those found in high temperature heat pumps or NH3/CO_2 cascade refrigeration systems. Dynamic pressure sensors were employed to measure the in-chamber pressure traces, an piezoresistive force sensors were installed at the discharge end of the male rotor to characterize the loads on the rolling bearings. Wang et al. [12] conducted numerical and experimental studies on the axis orbit of journal bearings. Experimental indicated diagrams were obtained in order to compute the gas-induced leads on the bearings by Finite Element Analysis (FEA).

The aim of this work is to employ a generalized simulation framework previously developed and validated by the authors for other positive displacement compressors to create a comprehensive twin-screw compressor model that includes all the necessary sub-models to predict the thermodynamic performance of the machine and quantify flow, heat, and friction

losses. Besides the modeling aspects, which have been widely covered in the literature, a fully instrumented open-drive twin-screw compressor will allow an in-depth validation of the model and break-down of the losses.

2. Mechanistic model

The comprehensive mechanistic model of the twin-screw compressor has been developed by employing the generalized modeling framework for positive displacement compressors developed by the authors [13]. The key elements of the model that are specific to the twin-screw compressor are briefly discussed in the following sections.

2.1. Governing equations

The compressor model is based on the thermodynamic concept of open-control volume to which mass and energy balance equations are applied. The control volume represents each of the compression chambers. In addition, static control volumes can be identified as the suction and discharge plenums. Such approach has been widely used to model positive displacement compressors including twin-screw compressors, as described by Stosic et al. [2]. As the compressor features oil-injection, a polygon intersection algorithm has been employed to obtain the effective injection port area. The oil flow rate is calculated by adopting a liquid nozzle flow model where the flow coefficient will have to be determined experimentally. An adaptive RK45 solver is used to integrate the set of differential equations over one working cycle.

The instantaneous pressure profile of the compression process is utilized to compute the gas compression force acting on the surface of the volume cavity at each rotation angle. The gas force is decomposed in axial and radial components that have to be balanced by sets of radial bearings and thrust bearings. A free body diagram of the rotor assembly is used to compute the loads of the bearings, as outlined by Stosic et al. [2].

The thermodynamic model and the force analysis are coupled with an overall energy balance of the compressor to calculate the discharge state. Furthermore, a four-pole method [14] is used a post-processing tool to compute the discharge gas pulsation in the discharge plenum.

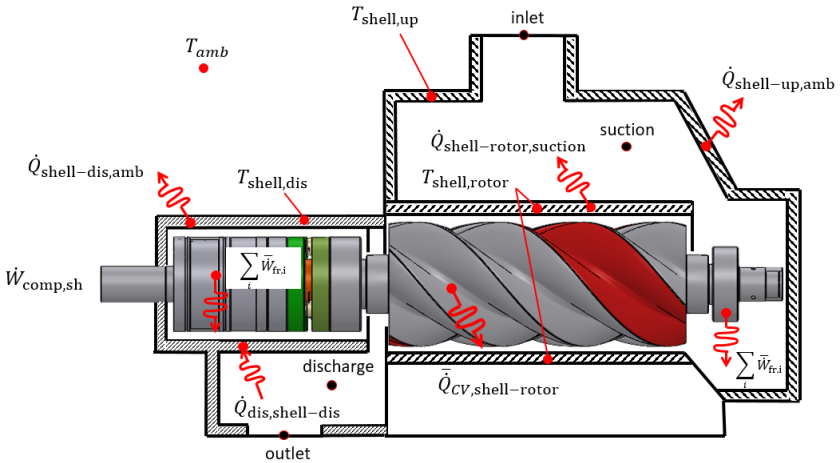


Figure 1. Schematic of the overall energy balance and thermal interactions in the twin-screw compressor.

2.2. Overall energy balance

The compressor model is closed with an overall energy balance to account for the different thermal interactions inside the machine. In the literature, several examples of thermal networks coupled with mechanistic models can be found [15, 16]. The compressor has been divided into different lumped masses and a multi-lumped steady-state thermal network has been identified. A schematic of the different lumped temperatures and the thermal flows is shown in Figure 1. The following energy balance equations can be derived to calculate the lumped temperatures that are unknown.

$$\dot{m}_{\mathrm{ref}}\left(h_{\mathrm{suc}}-h_{\mathrm{inlet}}\right)=\dot{Q}_{\mathrm{shell-rotor,suction}}-\dot{Q}_{\mathrm{suction,shell-up}}+\sum_{i}\overline{\dot{W}}_{\mathrm{fr,i}} \tag{1}$$

$$\dot{Q}_{\mathrm{shell,rotor}}-\overline{\dot{Q}}_{\mathrm{CV,shell-rotor}}=0 \tag{2}$$

$$\dot{Q}_{\mathrm{suction,shell-up}}-\dot{Q}_{\mathrm{shell-up,amb}}=0 \tag{3}$$

$$\dot{m}_{\mathrm{ref}}\left(h_{\mathrm{dis}}-h_{\mathrm{outlet}}\right)=\dot{Q}_{\mathrm{shell-dis,dis}} \tag{4}$$

$$\dot{Q}_{\mathrm{dis,shell-dis}}-\dot{Q}_{\mathrm{shell-dis,amb}}+\sum_{i}\overline{\dot{W}}_{\mathrm{fr,i}}=0 \tag{5}$$

where $\dot{Q}_{\mathrm{shell,rotor}}$, $\dot{Q}_{\mathrm{shell-rotor,suction}}$, $\dot{Q}_{\mathrm{suction,shell-up}}$, $\dot{Q}_{\mathrm{shell-up,amb}}$, $\dot{Q}_{\mathrm{shell-dis,amb}}$, $\dot{Q}_{\mathrm{dis,shell-dis}}$ are expressed in the following general form:

$$\dot{Q}=\frac{T_{\mathrm{a}}-T_{\mathrm{b}}}{R_{\mathrm{ab}}} \tag{6}$$

where T_{a} is the temperature difference between two lumped mass temperatures and $\mathrm{R_{ab}}$ is the heat transfer thermal resistance obtained by employing empirically correlated Nusselt numbers depending on the heat transfer process type.

2.3. Performance calculations

The most important integral quantities to be estimated by the model are the total mass flow rate delivered by the compressor, the oil injected mass flow rate, the indicated and total power, and the volumetric and isentropic efficiencies. The total refrigerant mass flow rate is given by the total mass within the compressor multiplied by the rotational speed of the male rotor:

$$\dot{m}_{\mathrm{ref}}=\frac{m_{\mathrm{ref}}z_1N_1}{60} \tag{7}$$

where m_{ref} is the actual mass within each cavity that accounts for leakage flows in and out the cavity. The theoretical mass flow rate is computed by knowing the maximum volume of the working chamber:

$$\dot{m}_{\mathrm{ref,th}}=\frac{(A_{01}+A_{02})L_{\mathrm{rotor}}\rho_{\mathrm{suc}}z_1N_1}{60} \tag{8}$$

where A_{01} and A_{02} are the cavity cross-section areas of male and female rotors, ρ_{suc} is the density of the working fluid at the suction conditions. Hence, the volumetric efficiency is given by:

$$\eta_{\mathrm{v}}=\frac{m_{\mathrm{ref}}}{\dot{m}_{\mathrm{ref,th}}} \tag{9}$$

Table 1. Twin-screw compressor main geometric parameters.

Parameter	**Units**	**Value**
Theoretical displacement	[cm^3/rev]	≈26000
Compressor volume ratio	[-]	2.0 - 4.1
Rotor wrap angle φ_w	[deg]	325
Male lobes, z_1	[-]	4
Female lobes, z_2	[-]	6
Center distance, $A_{O_1O_2}$	[m]	0.222
Rotor length, L_{rotor}	[m]	0.679
L_{rotor}/D_m	[-]	2.40

The indicated work transferred from the screw rotors during the suction, compression, and discharge processes is represented by the area of the indicated diagram (p-V) shown in Figure 17(b). Mathematically, the indicated work is expressed as:

$$W_{\text{comp,ind}} = \oint_{cycle} V dp \tag{10}$$

Within the indicated work, flow losses during the entire working cycle, leakages, heat exchange in the chambers as well as the influence of the injected oil are included. The resulting compressor indicated power is calculated as:

$$\dot{W}_{\text{comp,ind}} = \frac{W_{\text{comp,ind}} z_1 N_1}{60} \tag{11}$$

The indicated power of the compressor can also be obtained from numerical results by integrating the instantaneous torques on the rotor shafts over one working cycle, and summing up the contributions:

$$\dot{W}_{\text{comp,ind}} = \frac{2\pi N_1 \left(\tau_1 + \frac{z_1}{z_2}\tau_2\right)}{60} \tag{12}$$

The total compressor input power for an open-drive machine is given by summing the indicated power and the total friction losses:

$$\dot{W}_{\text{comp,sh}} = \dot{W}_{\text{comp,ind}} + \dot{W}_{\text{fr,loss}} \tag{13}$$

The frictional losses associated with the bearings are computed by knowing the axial and radial loads resulting from the decomposition of the gas compression forces. The overall isentropic efficiency is defined as:

$$\eta_{\text{is,oa}} = \frac{\dot{W}_{\text{comp,is}}}{\dot{W}_{\text{comp,tot}}} = \frac{\dot{m}_{\text{ref}} \left(h_{\text{dis,s}} - h_{\text{suc}}\right)}{\dot{W}_{\text{comp,sh}}} \tag{14}$$

Lastly, the mechanical efficiency of the open-drive compressor is given by:

$$\eta_{\text{comp,mech}} = \frac{\dot{W}_{\text{comp,ind}}}{\dot{W}_{\text{comp,sh}}} \tag{15}$$

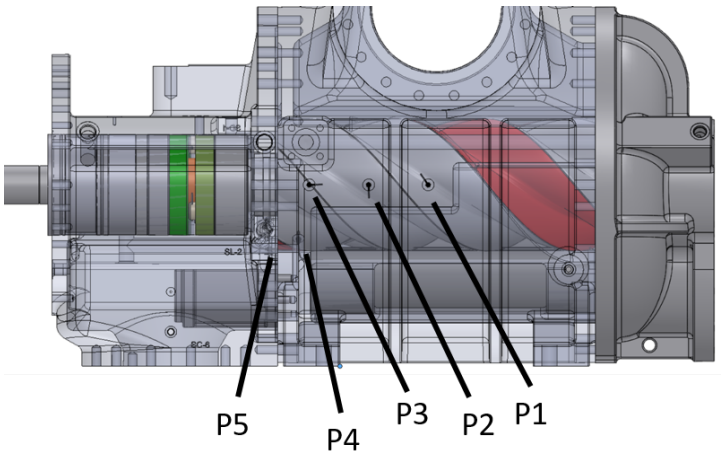
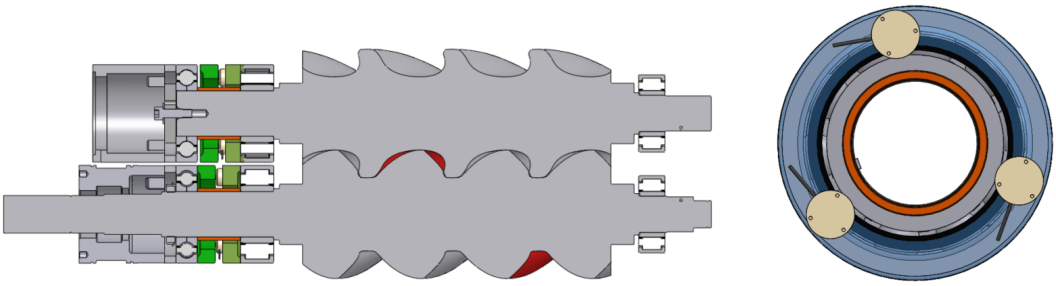


Figure 2. Side view of the twin-screw compressor showing the positioning of the internal pressure transducers.



(a) (b)

Figure 3. (*a*) 3D view of bearings on the suction and discharge sides and the assembly of the force transducers; (*b*) close-up view of the installation of the force transducers on the thrust bearings.

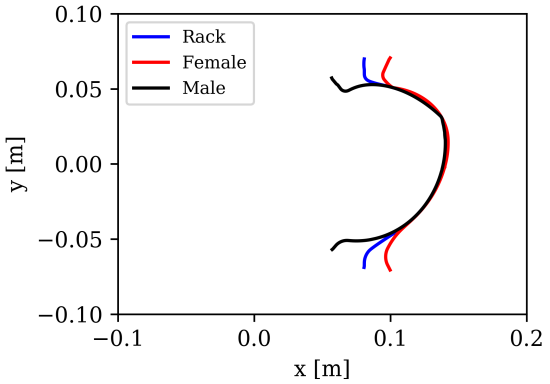
3. Test case

An open-drive twin-screw air-compressor with a 4/6 configuration has been selected as a test case. The main geometric parameters are listed in Table 1. The compressor is an oil-injected machine and the internal volume ratio is varied by meas of a sliding valve. In order to obtain detailed information about the operation of the compressor at both full- and part-load conditions, different internal measurements have been installed. In particular, high-frequency piezoelectric pressure transducers have been positioned along the rotor to capture the evolution of pressure during the compression process, as shown in Figure 2. A dedicated pressure transducer has been placed in the proximity of the discharge port to capture discharge pulsations. Piezoresistive sensors have been selected to measure the axial forces on the thrust bearings. The shaft configuration of the compressor can be seen in Figure 3(a). Ad-hoc designed mounting rings have installed between the radial and thrust bearings on the discharge end of the compressor on both shafts. Three force sensors have been places on the mounting rings and phased by 120°, as shown in Figure 3(b). In addition, thermocouples have been placed in different positions to measure the housing temperature variations. In order to measure the mechanical torque on the male shaft, a torque meter with an encoder has been installed between the compressor and the electric motor. A summary of the main sensors is provided in Table 2. The combination

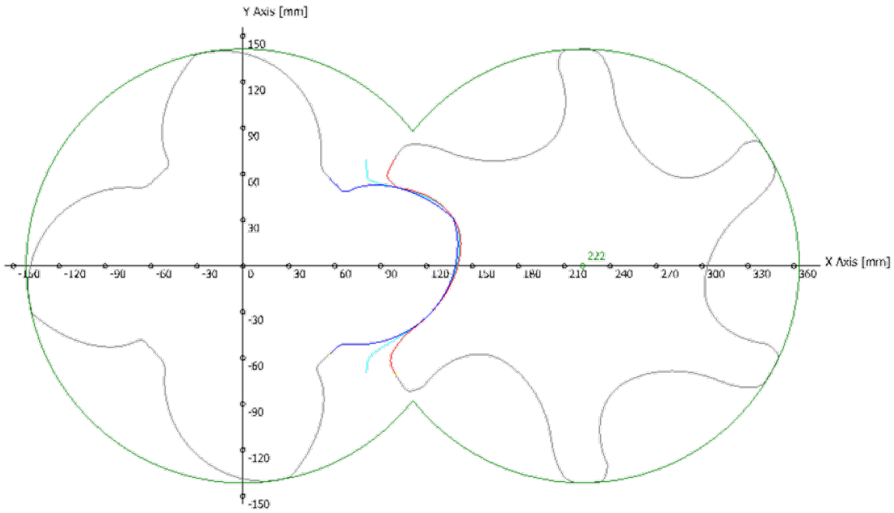
Table 2. List of installed internal sensors.

Measurement	Sensor Type	Accuracy
Dynamic Pressure	KULITE XTEL-190SM	±0.5% FSO (Max.)
Axial Force	Tacsis XLCH–005T-TS	±0.25% BFSL
Torque Meter	Lebow 1807-100K	±0.1% FS
Optical Tachometer	SPSR-115/230, 6150-020	

of internal pressure transducers, force sensors, and torque meter will allow to experimentally measure the frictional losses. Whereas, the housing temperature measurements will give an indication of the heat losses.



(a)



(b)

Figure 4. (*a*) Rack profile generated numerically; (*b*) verification of the rack profile by using the software SCORG [17].

4. Results and discussion

The theory of rack generation has been employed to recreate the male and female lobe profiles from a set of given points, as shown in Figure 4(a). In order to verify the calculations, SCORG

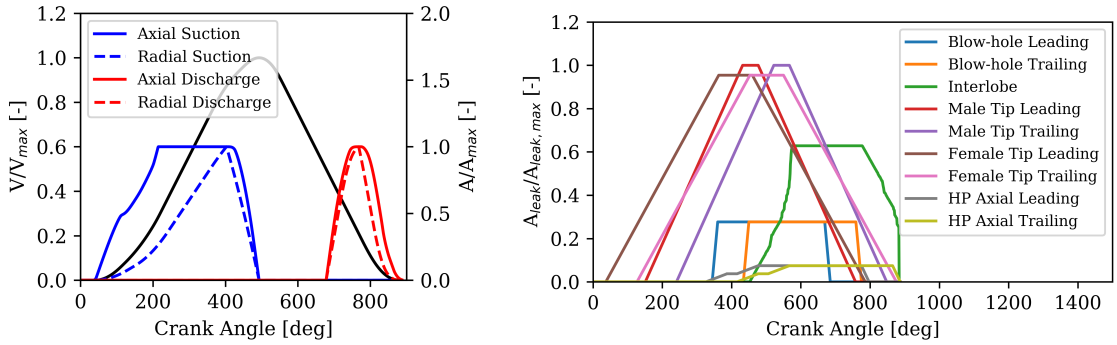


Figure 5. (a) Normalized cavity volume curve and suction and discharge port areas; (b) normalized leakage flow areas.

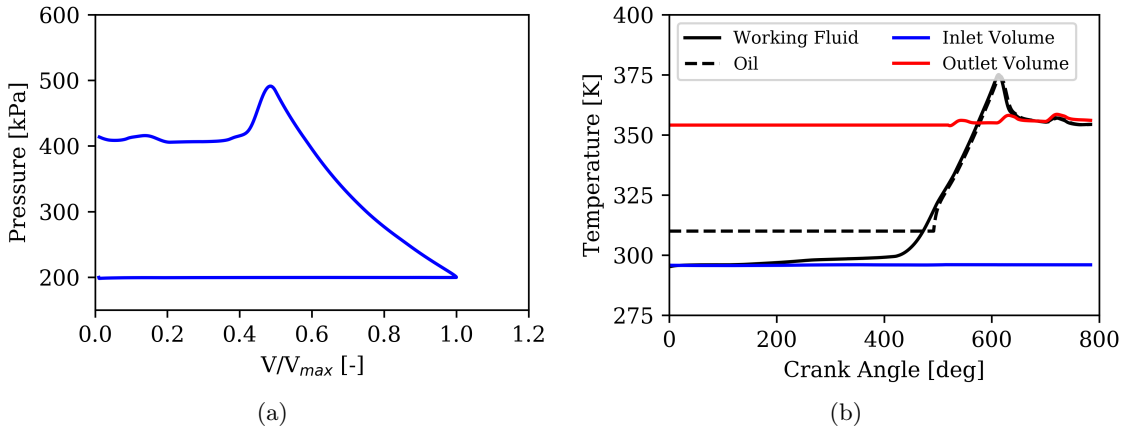


Figure 6. (a) Simulated indicated diagram; (b) evolution of working fluid and lubricant oil with male rotor rotation angle. The temperatures of the inlet and outlet volumes are also overlaid.

[17] has been employed to generate the numerical rack and the corresponding male and female profiles. The profiles were also compared with the mathematical model developed to ensure the correctness of the results. Based on the available literature, a geometry model has been implemented to compute working chamber volume, suction and discharge port areas, and leakage flow areas throughout the working process. In particular, Figure 5(a) shows the normalized curves for the working chamber volume and the suction and discharge port areas as a function of the crank-angle. Whereas, Figure 5(b) reports the normalized sealing lines and blow-holes as a function of the crank-angle. The twin-screw compressor model has been verified with the following set of operating conditions:

- working fluid: air;
- lubricant oil: polyalphaolefin (PAO) ISO Grade 68;
- male rotor rotational speed: 6000 rpm;
- suction pressure and temperature: 200 kPa, 295.15 K;
- pressure ratio: 2;
- oil injection inlet pressure and temperature: 300 kPa, 310.15 K.

The model provides insight on the working process of the compressor. In particular, the indicate diagram of the compression process is shown in Figure 6(a). The over-compression

losses are mitigated by employing the slide-valve mechanism, which is not shown here due to confidentiality. The temperature variations of the working fluid and the lubricant oil injected are reported in Figure 6(b). The temperature profiles of inlet and outlet chambers of the housing are also overlaid for completeness.

As previously mentioned, the pressure profile of each working chamber is utilized to compute the instantaneous compression loads, which are decomposed in axial and radial loads to be balanced by sets of bearings. The instantaneous total axial forces acting on the male and female rotors are shown in Figure 7(a). The radial loads on the low and high pressure sides of both male and female rotors are plotted in Figure 7(b). Finally, the shaft torques of male and female rotors can be seen in Figure 8(a). The indicated shaft torques are used to compute the indicated power as well as the actual shaft power once the frictional losses are included. The instantaneous power profiles are shown in Figure 8(b). As part of the ongoing experimental work, the magnitude and periodic behavior of the loads will be directly measured by the force transducers, which will also serve to validate the calculations. The total torque of the male rotor, i.e. indicated torque plus the frictional torque, are measured with a torque sensor. By measuring indicated diagram, axial loads, and the male shaft torque, the radial loads can also be obtained by applying the force and moments decomposition [2].

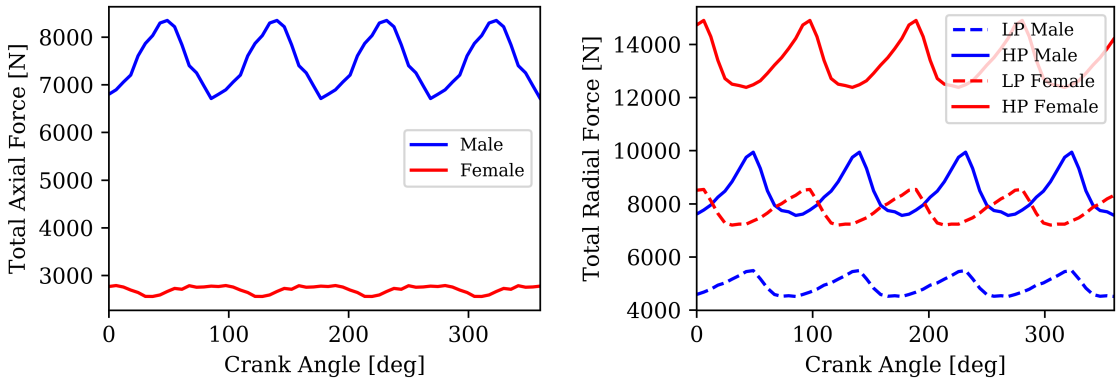


Figure 7. (*a*) Axial loads on male and female rotor shafts; (*b*) radial loads on male and female rotor shafts both on high- and low-side pressures.

5. Conclusions

In this paper, a comprehensive twin-screw compressor model has been introduced and utilized to compute the bearing loads on both male and female rotors. The model accounted for in-chamber thermodynamic processes including oil-injection, leakage flows, and heat transfer as well as the dynamic analysis of the forces acting on the rotors due the compression loads. The instantaneous results from the model have been shown. A twin-screw air compressor has been instrumented in internal sensors to record indicated diagram and axial forces on the thrust bearings along with a torque meter. The experimental data will be used to estimate the friction losses and validate the comprehensive model.

Acknowledgments

The authors would like to acknowledge the Center of High Performance Buildings (CHPB) for the financial support.

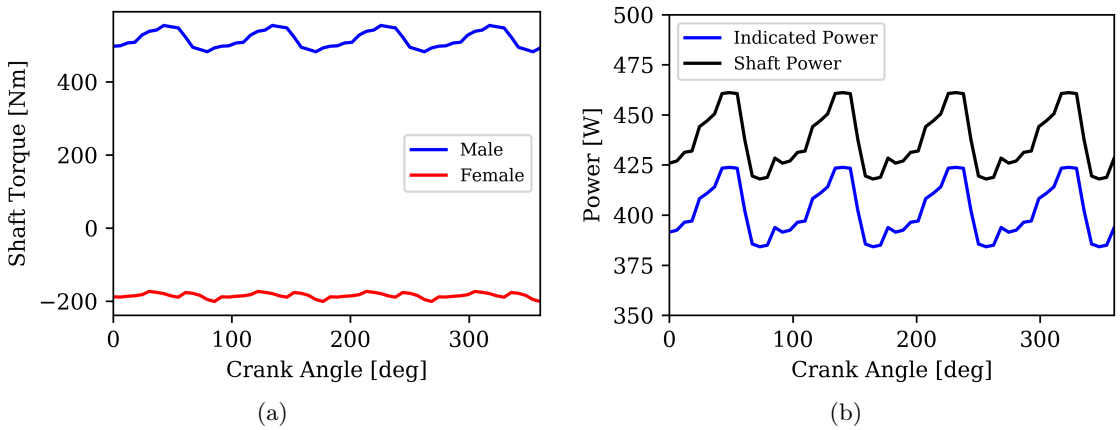


Figure 8. (*a*) Indicated shaft torque of male and female rotors; (*b*) instantaneous indicated and shaft power results.

References

[1] Tang Y 1994 *Computer aided design of twin screw compressors* Ph.D. thesis University of Strathclyde, Glasgow, UK

[2] Stosic N, Smith I and Kovacevic A 2005 *Screw Compressors - Mathematical Modelling and Performance Calculation* (Springer)

[3] Wu Y and Fong Z 2008 *Journal of Mechanical Design* **130** 1–8

[4] Wu Y and Fong Z 2009 *Mechanism and Machine Theory* **44** 66–82

[5] Zaytsev D and Infante Ferreira C 2005 *International Journal of Refrigeration* **28** 744–755

[6] Koai K 1990 *Mathematical modeling of twin screw compressors with special attention to gas pulsations in three-dimensional gas paths* Ph.D. thesis Purdue University

[7] Adams G 1993 *Modelling and computer simulation of rotor chatter and oscillating bearing forces in twin screw compressors* Ph.D. thesis Purdue University

[8] You C 1994 *A theoretical study of rotor forces and torques in helical twin screw compressors* Ph.D. thesis University of Strathclyde, Glasgow, UK

[9] Wu Y and Tran V 2016 *International Journal of Refrigeration* **65** 111–128

[10] Nikolov A and Brummer A 2017 *Energies* **10** 1–27

[11] Hou F, Zhao Z, Yu Z and Xing Z 2017 *International Journal of Refrigeration* **75** 155–163

[12] Wang C, Xing Z, Hou F, Wu H and Yu Z 2018 *International Journal of Refrigeration* **90** 1–11

[13] Bell I H, Ziviani D, Lemort V, Bradshaw C R, Mathison M M, Groll E A, Braun J E and Horton W T 2019 *International Journal of Refrigeration* **Submitted**

[14] Zhou W, Kim J and Soedel W 2001 *Journal of Mechanical Design* **123** 282–288

[15] Liu Z 1993 *Simulation of a Variable Speed Compressor with Special Attention to Supercharging Effects* Ph.D. thesis Purdue University

[16] Chen Y 2000 *Mathematical modeling of scroll compressors* Ph.D. thesis Purdue University

[17] PDM Analysis Ltd SCORG - Screw Compressor Rotor Grid Generator URL `http://pdmanalysis.co.uk/scorg/`